J|A|C|S
ARTICLES
Published on Web 01/13/2006

Substrate Specificity of an Active Dinuclear Zn(II) Catalyst for Cleavage of RNA Analogues and a Dinucleoside

AnnMarie O'Donoghue,[†] Sang Yong Pyun,[‡] Meng-Yin Yang,[†] Janet R. Morrow,*[,†] and John P. Richard*[,†]

Contribution from the Departments of Chemistry, University at Buffalo, State University of New York, Buffalo, New York 14260-3000 and Pukyong National University, Busan 608-737, Korea

Received September 7, 2005; E-mail: jmorrow@buffalo.edu; jrichard@buffalo.edu

Abstract: The cleavage of the diribonucleoside **UpU** (uridylyl-3′-5′-uridine) to form uridine and uridine (2′,3′)-cyclic phosphate catalyzed by the dinuclear Zn(II) complex of 1,3-bis(1,4,7-triazacyclonon-1-yl)-2-hydroxypropane (**Zn_2(1)(H_2O)**) has been studied at pH 7−10 and 25 °C. The kinetic data are consistent with the accumulation of a complex between catalyst and substrate and were analyzed to give values of k_c (s^{-1}), K_d (M), and k_c/K_d (M^{-1} s^{-1}) for the **Zn_2(1)(H_2O)**-catalyzed reaction. The pH rate profile of values for log k_c/K_d for **Zn_2(1)(H_2O)**-catalyzed cleavage of **UpU** shows the same downward break centered at pH 7.8 as was observed in studies of catalysis of cleavage of 2-hydroxypropyl-4-nitrophenyl phosphate (**HpPNP**) and uridine-3′-4-nitrophenyl phosphate (**UpPNP**). At low pH, where the rate acceleration for the catalyzed reaction is largest, the stabilizing interaction between **Zn_2(1)(H_2O)** and the bound transition states is 9.3, 7.2, and 9.6 kcal/mol for the catalyzed reactions of **UpU**, **UpPNP**, and **HpPNP**, respectively. The larger transition-state stabilization for **Zn_2(1)(H_2O)**-catalyzed cleavage of **UpU** (9.3 kcal/mol) compared with **UpPNP** (7.2 kcal/mol) provides evidence that the transition state for the former reaction is stabilized by interactions between the catalyst and the C-5′-oxyanion of the basic alkoxy leaving group.

Introduction

In recent years attempts to design and synthesize low molecular weight catalysts with activities that approach those of protein and RNA catalysts have produced many significant and interesting results[1−17] but no major breakthroughs. This may be a sign that large molecular weights are somehow essential to the construction of catalysts that show a high degree of complementarity to the transition state for the catalyzed reaction. On the other hand, it is early to conclude that the limits are being approached for the activity of small molecule catalysts.

We have shown that the small molecule dinuclear zinc complex **Zn_2(1)(H_2O)** gives a transition-state stabilization for catalysis of cleavage of the simple phosphodiester 2-hydroxypropyl-4-nitrophenyl phosphate (**HpPNP**) that is a substantial fraction (≤50%) of the maximum possible for a hypothetical protein or ribozyme catalyst of the same reaction.[18,19] **Zn_2(1)(H_2O)** owes its high activity to cooperative interactions between the tethered Zn(II) cations and the linker alkoxide anion, which draw the cations into a densely charged core that interacts effectively with the anionic transition state for phosphodiester cleavage.[19−23] We want to extend this characterization of the unusual catalytic power of **Zn_2(1)(H_2O)** to the cleavage of ribonucleic acids in order to obtain insight into the origin of the rate accelerations for metalloenzyme-[24] and ribozyme-catalyzed[25,26] cleavage of RNA and because a better understanding of what limits the catalytic power of **Zn_2(1)(H_2O)** will help

[†] State University of New York, Buffalo.
[‡] Pukyong National University.

(1) Wall, M.; Hines, R.; Chin, J. *Angew. Chem., Int. Ed. Engl.* **1993**, *32*, 1633−1635.
(2) Young, M. J.; Chin, J. *J. Am. Chem. Soc.* **1995**, *117*, 10577−10578.
(3) Liu, S.; Hamilton, A. D. *Tetrahedron Lett.* **1997**, *38*, 1107−1110.
(4) Molenveld, P.; Engbersen, J. F. J.; Kooijman, H.; Spek, A. L.; Reinhoudt, D. N. *J. Am. Chem. Soc.* **1998**, *120*, 6726−6737.
(5) Liu, S.; Hamilton, A. D. *Bioorg. Med. Chem. Lett.* **1997**, *7*, 1779−1784.
(6) Fritsky, I. O.; Ott, R.; Pritzkow, H.; Kramer, R. *Inorg. Chim. Acta* **2003**, *346*, 111−118.
(7) Fritsky, I. O.; Ott, R.; Pritzkow, H.; Kramer, R. *Chem. Eur. J.* **2001**, *7*, 1221−1231.
(8) Gajda, T.; Jancso, A.; Mikkola, S.; Lonnberg, H.; Sirges, H. *J. Chem. Soc., Dalton Trans.* **2002**, 1757−1763.
(9) Gajda, T.; Kramer, R.; Jancso, A. *Eur. J. Inorg. Chem.* **2000**, 1635−1644.
(10) Chapman, W. H., Jr.; Breslow, R. *J. Am. Chem. Soc.* **1995**, *117*, 5462−5469.
(11) Yashiro, M.; Ishikubo, A.; Komiyama, M. *J. Chem. Soc., Chem. Commun.* **1995**, 1793−1794.
(12) Yashiro, M.; Ishikubo, A.; Komiyama, M. *J. Chem. Soc., Chem. Commun.* **1997**, 83−84.
(13) Rossi, P.; Felluga, F.; Tecilla, P.; Formaggio, F.; Crisma, M.; Toniolo, C.; Scrimin, P. *J. Am. Chem. Soc.* **1999**, *121*, 6948−6949.
(14) Albedyhl, S.; Averbuch-Pouchot, M. T.; Belle, C.; Krebs, B.; Pierre, J. L.; Saint-Aman, E.; Torelli, S. *Eur. J. Inorg. Chem.* **2001**, 1457−1464.
(15) Albedyhl, S.; Schnieders, D.; Jancso, A.; Gajda, T.; Krebs, B. *Eur. J. Inorg. Chem.* **2002**, 1400−1409.
(16) Williams, N. H.; Cheung, W.; Chin, J. *J. Am. Chem. Soc.* **1998**, *120*, 8079−8087.
(17) Williams, N. H.; Takashi, B.; Wall, M.; Chin, J. *Acc. Chem. Res.* **1999**, *32*, 485−493.
(18) Morrow, J.; Iranzo, O. *Curr. Opin. Chem. Biol.* **2004**, *8*, 192−200.
(19) Iranzo, O.; Kovalevsky, A. Y.; Morrow, J. R.; Richard, J. P. *J. Am. Chem. Soc.* **2003**, *125*, 1988−1993.
(20) Iranzo, O.; Elmer, T.; Richard, J. P.; Morrow, J. R. *Inorg. Chem.* **2003**, *42*, 7737−7746.
(21) Yang, M.-Y.; Richard, J. P.; Morrow, J. R. *Chem. Commun.* **2003**, 2832−2833.
(22) Iranzo, O.; Richard, J. P.; Morrow, J. R. *Inorg. Chem.* **2004**, *43*, 1743−1750.
(23) Yang, M.-Y.; Iranzo, O.; Richard, J. P.; Morrow, J. R. *J. Am. Chem. Soc.* **2005**, *127*, 1064−1065.
(24) Cowan, J. A. *Chem. Rev.* **1998**, *98*, 1067−1087.
(25) Kuimelis, R. G.; McLaughlin, L. W. *Chem. Rev.* **1998**, *98*, 1027−1044.
(26) Zhou, D.-M.; Taira, K. *Chem. Rev.* **1998**, *98*, 991−1026.

Scheme 1

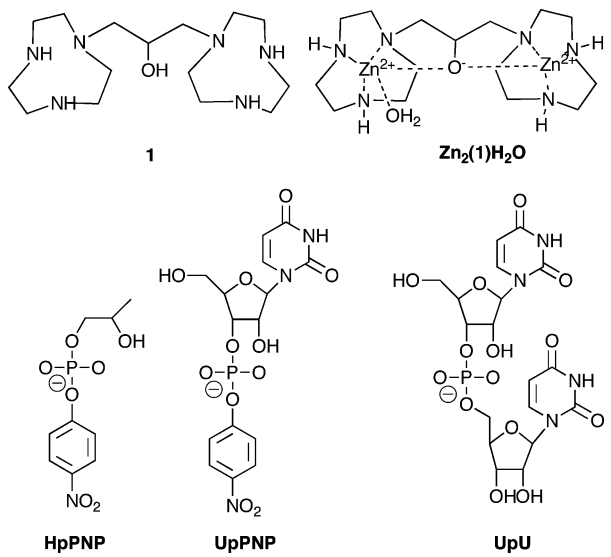

to guide the rational incorporation of design elements to overcome these limits.

Chromophoric substrates were used in earlier studies on **Zn_2(1)(H_2O)** because of the ease of monitoring reactions by UV spectroscopy.[19−23] The 4-nitrophenoxide ion leaving group of **HpPNP** and uridine-3′-4-nitrophenyl phosphate (**UpPNP**) is weakly basic and intramolecular addition of the C-2′ ribosyl oxyanion to the substrate phosphate must be rate determining if the reactions proceed by a stepwise mechanism through an oxyphosphorane dianion reaction intermediate.[27] RNA differs from **HpPNP** and **UpPNP** in that the C-5′ alkoxy oxygen of the nucleoside leaving group is strongly basic. Therefore, breakdown of the intermediate with expulsion of the leaving group anion will be the rate-determining step, if the reaction mechanism is stepwise, or there will be partial cleavage of the bond to the leaving group and development of negative charge at oxygen, if the reaction mechanism is concerted.[26−31] In either case stabilization of negative charge at this leaving oxygen at the rate-determining transition state might contribute to the rate acceleration for **Zn_2(1)(H_2O)**-catalyzed cleavage of RNA but not for the catalyzed reactions of **HpPNP** and **UpPNP**.[32] We therefore extended our studies on **Zn_2(1)(H_2O)** to the ribodinucleotide substrate **UpU** in which the leaving group is the same as for RNA to determine if an enhanced rate acceleration is observed for this substrate that is consistent with a stabilizing electrostatic interaction between the catalyst and the strongly basic anionic leaving group

We report here kinetic parameters over a broad range of pH for the cleavage of **UpU** (Scheme 1) catalyzed by **Zn_2(1)(H_2O)** and a comparison of these data with the corresponding parameters for **Zn_2(1)(H_2O)**-catalyzed cleavage of **HpPNP**[19] and **UpPNP**.[21] Our data show that **Zn_2(1)(H_2O)** provides 2.1 kcal/mol greater stabilization of the transition state for the cleavage of **UpU**, where the leaving group is strongly basic, than of the transition state for the cleavage of **UpPNP**, where the leaving group is the weakly basic 4-nitrophenoxide ion. This provides evidence for a modest stabilization of negative charge at the leaving group of **UpU** by interaction with **Zn_2(1)(H_2O)**. We also present a comparison of the specificity of **Zn_2(1)(H_2O)** for catalysis of the cleavage reactions of **HpPNP**, **UpPNP**, and **UpU** as measured by the net stabilization by the catalyst of the transition state for the uncatalyzed reaction, which provides insight into the strengths and limitations of **Zn_2(1)(H_2O)** as a catalyst of phosphate diester cleavage.

Experimental Section

All buffers, $Zn(NO_3)_2$, uridylyl(3′,5′)uridine (**UpU**, NH_4^+ salt), uridine (2′,3′)-cyclic monophosphate (2′,3′-*c*UMP), uridine-3′-monophosphate (3′-UMP), uridine 2′-monophosphate (2′-UMP), uridine, and uracil were reagent grade from Sigma-Aldrich. Water was distilled and then passed through a Milli-Q purification system. The ligand **1** was prepared by literature procedures.[20,33,34] A stock solution of **UpU** was shown to be stable to cleavage for a period of several weeks at neutral pH. The solution pH was determined at 25 °C using an Orion digital pH meter equipped with a temperature compensation probe. Procedures described in earlier work were used in preparing solutions of **Zn_2(1)(H_2O)** for kinetic studies.[19]

HPLC Product Analysis. The cleavage of **UpU** was monitored by separating the reactant and products over a C18 radial-pak column (250 mm × 4.6 mm) using a Waters 600E HPLC equipped with a 490 UV−Vis detector with peak detection at 260 nm. An isocratic elution solvent, prepared by mixing nine parts water at pH 4.3 (60 mM acetic acid buffer and 0.10 M NH_4Cl) with one part methanol, was used for all separations. The sodium salt of *p*-nitrobenzenesulfonate was included with all samples as an internal standard to allow for corrections in small variations in the volume of the sample injected. The reactant **UpU** and products 2′,3′-*c*UMP, 3′-UMP, 2′-UMP, and uridine were identified by comparison of retention times with those of authentic material. The extinction coefficients at 260 nm, relative to a standard value of 1.0 for uracil, were determined from the ratio of concentrations and peak areas from HPLC analysis of known concentrations of the following compounds: uracil, 1.00; 2′,3′-*c*UMP, 1.06; 3′-UMP, 0.91; 2′-UMP, 0.96; uridine, 1.19; UpU, 2.32.

Kinetic Measurements. The following buffers were used for these experiments: imidazole, pH 7.0−7.4; 2-(*N*-cyclohexylamino)ethanesulfonic acid (CHES), pH 8.9−9.3; 3-(cyclohexylamino)-1-propanesulfonic acid (CAPS), pH 9.8. The solutions used for kinetic analyses were prepared by mixing measured amounts of **UpU**, **Zn_2(1)(H_2O)**, ,*p*-nitrobenzene-sulfonate ion and the appropriate buffer to give final concentrations of 0.070 mM **UpU**, 0−2.00 mM **Zn_2(1)(H_2O)**, 0.020 mM *p*-nitrobenzenesulfonate ion, and 20 mM buffer at $I = 0.10$ ($NaNO_3$) in a volume of 0.50 mL. The solution was kept at 25 °C; at measured times 50 μL aliquots were withdrawn, the pH adjusted to 4−5 with a small volume of acetate buffer; the relative concentrations of substrate **UpU** and products were determined by HPLC analysis. First-order rate constants k_{obsd} (s^{-1}) were determined as the slopes of linear plots of reaction progress against time over the first 2−8% reaction using eq 1, where [Uridine] is the concentration of the cleavage product and $[UpU]_o$ is the initial concentration of the substrate. Rate constants for the solvent-catalyzed reaction were determined under the same conditions but in the absence of **Zn_2(1)(H_2O)**. Linear and nonlinear least-squares fits of kinetic data to the appropriate kinetic equations were performed using SigmaPlot from Jandel Scientific.

$$\frac{[\text{Uridine}]}{[\text{UpU}]_o} = k_{obsd}t \qquad (1)$$

(27) Perreault, D. M.; Anslyn, E. V. *Angew. Chem., Int. Ed. Engl.* **1997**, *36*, 432−450.
(28) Skoog, M. T.; Jencks, W. P. *J. Am. Chem. Soc.* **1984**, *106*, 7597−7606.
(29) Stefanidis, D.; Cho, S.; Dhe-Paganon, S.; Jencks, W. P. *J. Am. Chem. Soc.* **1993**, *115*, 1650−1656.
(30) Lonnberg, H.; Stromberg, R.; Williams, A. *Org. Biomol. Chem.* **2004**, *2*, 2165−2167.
(31) Davis, A. M.; Hall, A. D.; Williams, A. *J. Am. Chem. Soc.* **1988**, *110*, 5105−5108.
(32) Menger, F. M.; Ladika, M. *J. Am. Chem. Soc.* **1987**, *109*, 3145−3146.

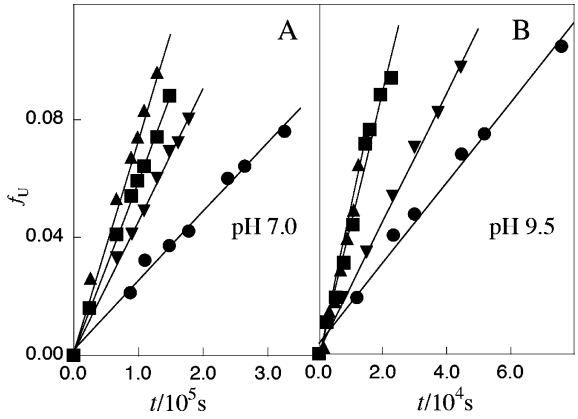

Figure 1. Increase in the fractional conversion of **UpU** to uridine (f_U) with time for **Zn_2(1)(H_2O)**-catalyzed reactions at 25 °C. The slope of these linear correlations is equal to k_{obsd} (s^{-1}) for the **Zn_2(1)(H_2O)**-catalyzed reaction. (A) Reactions at pH 7.0: (●) 0.5 mM, (▼) 1.0 mM, (■) 1.5 mM, (▲) 2.0 mM [**Zn_2(1)(H_2O)**]$_T$. (B) Reactions at pH 9.5: (●) 0.25 mM, (▼) 0.50 mM, (■) 1.5 mM, (▲) 2.0 mM **Zn_2(1)(H_2O)**.

Results

The cleavage of **UpU** (0.070 mM) catalyzed by **Zn_2(1)(H_2O)** at 25 °C and pH 7.0−9.8 maintained with 20 mM of the appropriate buffer at $I = 0.10$ M ($NaNO_3$) was monitored by HPLC. These analyses showed that this reaction gives uridine and 2′,3′-*c*UMP as products at early times and that 2′,3′-*c*UMP undergoes hydrolysis to 3′-UMP and 2′-UMP at longer times.

The kinetic parameters for the cleavage of **UpU** catalyzed by **Zn_2(1)(H_2O)** were determined by monitoring the disappearance of **UpU** and the formation of uridine by HPLC. Figure 1 shows representative plots of the fractional conversion of **UpU** to uridine (f_U) with time during the initial stages of reactions at pH 7.0 and 9.5 (25 °C). The different solid lines show data for reactions catalyzed by different [**Zn_2(1)(H_2O)**]$_T$, where [**Zn_2(1)(H_2O)**]$_T$ is the sum of the concentrations of the catalyst in the protonated ([**Zn_2(1)(H_2O)**]) and ionized ([**Zn_2(1)(HO^-)**]) forms (see below). Values of k_{obsd} for the reactions of **UpU** were calculated from the slopes of these linear correlations (eq 1).

$$k_{obsd} = \left[\frac{k_c[\mathbf{Zn_2(1)(H_2O)}]_T}{K_d + [\mathbf{Zn_2(1)(H_2O)}]_T}\right] \qquad (2)$$

Figure 2 shows the increase in k_{obsd} for the cleavage of **UpU** as [**Zn_2(1)(H_2O)**]$_T$ is increased from 0 to 2.0 mM for reactions at 25 °C, pH 7.0−9.8, 20 mM buffer, and $I = 0.10$ ($NaNO_3$). The downward curvature observed for these plots is consistent with the formation of a complex between substrate **UpU** and catalyst **Zn_2(1)(H_2O)**. The solid lines through the experimental data in Figure 2 show the fit from nonlinear least-squares analysis of the experimental data to eq 2 derived for Scheme 2. Table 1 lists the kinetic parameters k_c (s^{-1}), K_d (M), and $(k_c/K_d)_{app}$ (M^{-1} s^{-1}) determined by this fitting procedure. The values of K_d (Table 1) are >10-fold larger than [**UpU**] = 0.070 mM (Table 1). Under these conditions >90% of the catalyst will be in the free form ([[**Zn_2(1)(H_2O)**]$_T$] ≫ [[**Zn_2(1)(H_2O)**]$_T$·**UpX**], Scheme 2) for reactions at all concentrations of **Zn_2(1)(H_2O)** (≥0.1 mM) used in these experiments as was assumed in the derivation of eq 2.

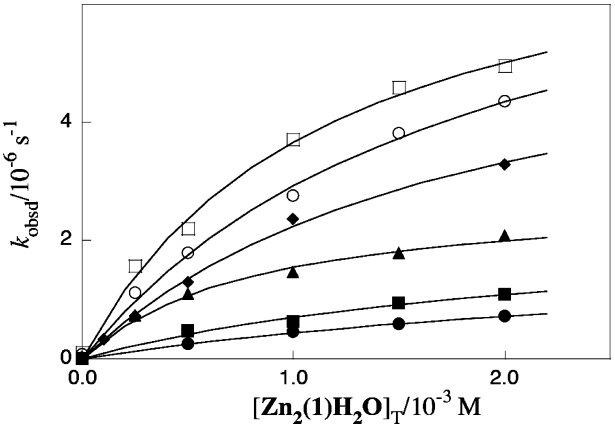

Figure 2. Effect of increasing concentrations of catalyst **Zn_2(1)(H_2O)** on the observed first-order rate constant k_{obsd} for cleavage of **UpU** at 25 °C. The solid lines show the nonlinear least-squares fit of the experimental data to eq 2 derived for Scheme 2. Reactions at pH 7.0 (●), 7.4 (■), 8.9 (▲), 9.3 (◆), 9.5 (○), 9.8 (□).

Scheme 2

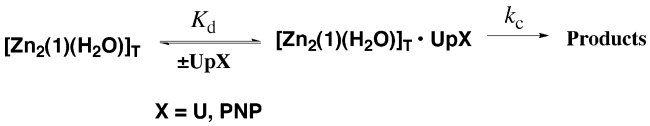

Table 1. Kinetic Parameters K_d, k_c, and $(k_c/K_d)_{app} = (k_{Zn})_{app}$ for **Zn_2(1)(H_2O)**-Catalyzed Cleavage of **UpU** at 25 °C

pH	$(k_{Zn})_{app}$[a] M^{-1} s^{-1}	K_d/mM[b,d]	$k_c/10^{-6}$ s^{-1} [c,d]
7.0	0.00056	3.5 ± 0.5	2.0 ± 0.2
7.4	0.00099	2.4 ± 0.9	2.4 ± 0.6
8.9	0.0034	0.80 ± 0.13	2.8 ± 0.2
9.3	0.0035	1.9 ± 0.3	6.4 ± 0.3
9.5	0.0045	1.9 ± 0.3	8.4 ± 1.0
9.8	0.0068	1.2 ±0.01	7.9 ± 0.6

[a] Apparent second-order rate constant for the **Zn_2(1)(H_2O)**-catalyzed reaction, calculated as the ratio k_c/K_d. [b] Dissociation constant of the substrate for **Zn_2(1)(H_2O)** calculated from the nonlinear least-squares fit of the data from Figure 2 to eq 2 derived for Scheme 2. [c] Limiting rate constant at high concentrations of **UpU** calculated from the nonlinear least-squares fit of the data from Figure 2 to eq 2 derived for Scheme 2. [d] The uncertainties in these kinetic parameters are from the nonlinear least-squares analysis of the data.

Linear plots of k_{obsd} against the catalyst concentration [≤2 mM] were observed for **Zn_2(1)(H_2O)**-catalyzed cleavage of the chromophoric substrate **UpPNP** at pH 7.0.[21] Figure 3 shows that there is a small downward curvature in the plot of k_{obsd} against [**Zn_2(1)(H_2O)**] for cleavage of **UpPNP** as the concentration of the catalyst is increased to 6.0 mM. The solid line through the experimental data in Figure 3 shows the fit from nonlinear least-squares analysis of the experimental data to eq 2 derived for Scheme 2 using values of $K_d = 9$ mM and $k_c = 0.31$ s^{-1}.

Apparent second-order rate constants $(k_{Zn})_{app}$ (M^{-1} s^{-1}) for **Zn_2(1)(H_2O)**-catalyzed cleavage of **UpU** were determined as $(k_{Zn})_{app} = (k_c/K_d)_{app}$ (Table 1). These second-order rate constants have the same physical significance as second-order rate constants $(k_{Zn})_{app}$ (M^{-1} s^{-1}) reported in earlier studies of **Zn_2(1)(H_2O)**-catalyzed cleavage of **UpPNP**[21] and **HpPNP**,[19,20,22] which were determined as the slopes of linear plots of k_{obsd} against [**Zn_2(1)(H_2O)**]$_T$. Figure 4 shows a plot of log$(k_c/K_d)_{app} = (k_{Zn})_{app}$ for **Zn_2(1)(H_2O)**-catalyzed cleavage of **UpU** and the plot of log$(k_{Zn})_{app}$ against pH for **Zn_2(1)(H_2O)**-catalyzed

(33) McCue, D. P. Ph.D. Thesis, University at Buffalo, SUNY: Buffalo, 1999.
(34) Atkins, T. J.; Richman, J. E.; Oettle, W. F. *Org. Synth.* **1978**, *58*, 86−98.

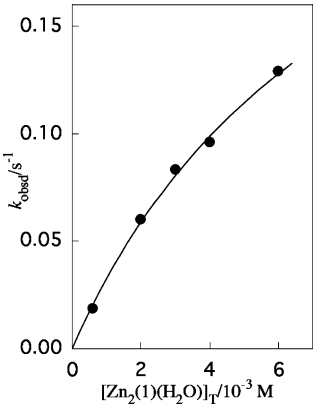

Figure 3. Effect of increasing concentrations of catalyst **Zn_2(1)(H_2O)** on the observed first-order rate constant k_{obsd} for cleavage of **UpPNP** for reactions at 25 °C and pH 7.0. The solid lines show the nonlinear least-squares fit of the experimental data to eq 2 derived for Scheme 2.

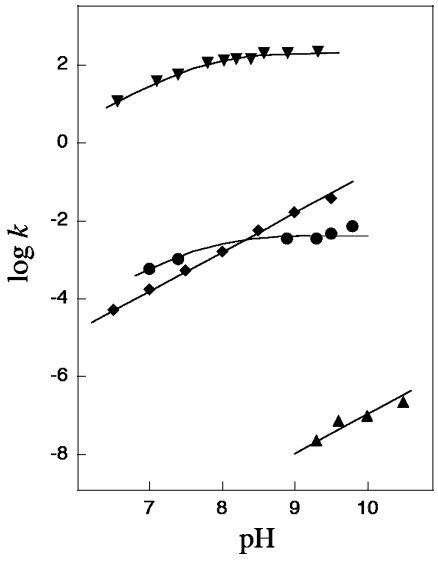

Figure 4. pH rate profiles of second-order rate constants k_{HO} and $(k_{Zn})_{app}$ for cleavage of phosphodiester substrates **UpPNP** and **UpU** catalyzed by hydroxide ion and **Zn_2(1)(H_2O)**. **UpPNP** [data from ref 21]: (◆) k_{HO}, (▼) $(k_{Zn})_{app}$. **UpU**: (▲) k_{HO}, (●) $(k_{Zn})_{app}$. The solid lines through values for $(k_{Zn})_{app}$ show the theoretical fits of the data to eq 3 derived for Scheme 3.

cleavage of **UpPNP** taken from earlier work.[21] The solid lines through these two sets of experimental data were drawn using eq 3 derived for Scheme 3 and values of $k_{Zn} = 0.005$ and 200 $M^{-1}s^{-1}$, respectively, for **Zn_2(1)(H_2O)**-catalyzed cleavage of **UpU** and **UpPNP**[21] and a pK_a of 7.8.[21,22] The value of pK_a = 7.8 determined from the nonlinear least-squares fit of kinetic data for the reactions of **UpPNP**[21] and **HpPNP**[19] is in agreement with the value of pK_a = 8.0 determined by potentiometric titration.[19] The value of $(k_{Zn})_{app} = (k_c/K_d)_{app} = 34$ M^{-1} s^{-1} for **Zn_2(1)(H_2O)**-catalyzed cleavage of **UpPNP** at pH = 7.0 calculated from the kinetic parameters determined for Figure 3 is in agreement (±10%) with $(k_{Zn})_{app} = 27$ M^{-1} s^{-1} that can be calculated from eq 3 using 200 M^{-1} s^{-1} and $K_a = 10^{-7.8}$ M.[21]

$$(k_{Zn})_{app} = (k_c/K_d)_{app} = \left[\frac{k_{Zn}K_a}{K_a + [H^+]}\right] \qquad (3)$$

Figure 4 also shows the pH rate profiles of the observed first-order rate constants for spontaneous cleavage of **UpU** and **UpPNP**.[21] Both cleavage reactions are first order in the concentration of hydroxide ion. The solid line through the experimental data shows the fits of the experimental data obtained using values of $k_{HO} = 0.0011$ and 1600 M^{-1} s^{-1}, respectively, for hydroxide-ion-catalyzed cleavage of **UpU** and **UpPNP** determined by nonlinear least-squares analyses.

Scheme 3

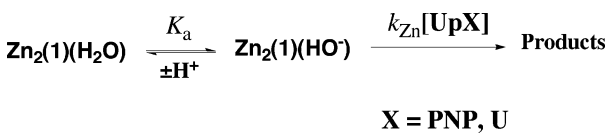

Discussion

The cleavage of **UpU** and related diribonucleosides is very slow at room temperature, and these reactions are therefore normally studied at elevated temperature.[35−38] The efficient catalysis of cleavage of **UpU** by **Zn_2(1)(H_2O)** allows us to study this reaction at the same temperature (25 °C) used for earlier studies on **Zn_2(1)(H_2O)**-catalyzed cleavage of **HpPNP**[19] and **UpPNP**.[21] The apparent second-order rate constants $\log(k_c/K_d)_{app} = (k_{Zn})_{app}$ for **Zn_2(1)(H_2O)**-catalyzed cleavage of **UpU** are first order in hydroxide ion at neutral pH and show a downward break centered at pH = pK_a = 7.8 for ionization of **Zn_2(1)(H_2O)** to **Zn_2(1)(HO^-)**. The same pH dependence was reported in earlier work for **Zn_2(1)(H_2O)**-catalyzed reactions of **HpPNP**[19] and **UpPNP**.[21] This shows that each of these three catalyzed reactions proceeds by reaction of the same ionic forms of substrate and catalyst.[23] The data in Table 1 suggest that there is both a small decrease in K_d and an increase in k_c with increasing pH; however, the scatter in the data is large. These changes provide evidence that both the ground-state complex between substrate and catalyst and the transition state for conversion of this complex to products are stabilized at increasing pH. The discussion in this paper will focus on the larger changes in $(k_{Zn})_{app} = (k_c/K_d)_{app}$ for which a good correlation with changing pH is observed.

Substrate Specificity. The large rate accelerations achieved by enzyme catalysts are due to the high degree of complementarity between the protein and the transition state for the catalyzed reaction. This generally results in a high *specificity* of the protein for binding to the transition state.[39−41] **Zn_2(1)(H_2O)** is a very effective catalyst for the cleavage of **HpPNP** and achieves ≈50% of the reduction in the activation barrier for the uncatalyzed reaction (transition-state stabilization) that would be observed for optimal enzymatic catalysis of this reaction.[19] Small molecule catalysts such as **Zn_2(1)(H_2O)** do not have the well-defined binding pocket required to show a high degree of complementarity for the transition state for the cleavage of **HpPNP** or cleavage of any other phosphate diester. However, the tight binding of **Zn_2(1)(H_2O)** to the transition state for phosphodiester cleavage reflects in some sense the specificity of the catalyst for transition-state binding, and this specificity can be determined through an examination of the transition-state stabilization for catalysis of reactions of different substrates.

One measure of substrate specificity of **Zn_2(1)(H_2O)** is the binding energy observed upon transfer of the transition state of the uncatalyzed reaction from solution to the catalyst.[39,41]

(35) Anslyn, E.; Breslow, R. *J. Am. Chem. Soc.* **1989**, *111*, 4473−4482.
(36) Kirby, A. J.; Marriott, R. E. *J. Am. Chem. Soc.* **1995**, *117*, 833−834.
(37) Kiviniemi, A.; Lonnberg, T.; Ora, M. *J. Am. Chem. Soc.* **2004**, *126*, 11040−11045.

Scheme 4

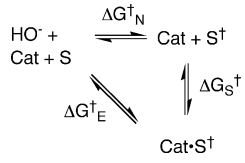

$$\Delta G_S^{\dagger} = \Delta G_E^{\dagger} - \Delta G_N^{\dagger} = -RT \ln\left[\frac{k_{Zn}K_a/K_w}{k_{HO}}\right] \qquad (4)$$

Table 2. Kinetic Parameters for **Zn_2(1)(H_2O)-** and Hydroxide-Ion-Catalyzed Cleavage of **HpPNP**, **UpPNP**, and **UpU** at 25 °C

	HpPNP[a]	UpPNP[b]	UpU[c]
k_{Zn} (M^{-1} s^{-1})[d]	0.71	200	0.005
($k_{Zn}K_a/K_w$) (M^{-2} s^{-1})[e]	1.1×10^6	3.2×10^8	8×10^3
k_{HO} (M^{-1} s^{-1})[f]	0.099	1600	0.0011
($k_{Zn}K_a/K_w$)/k_{HO} (M^{-1})[g]	1.1×10^7	2.0×10^5	7×10^6
$(\Delta G_S^{\dagger})_{max}$[h] (kcal/mol)	−9.6	−7.2	−9.3

[a] Data from ref 19. [b] Data from ref 21. [c] This work. [d] Limiting second-order rate constant observed for the **Zn_2(1)(H_2O)**-catalyzed reaction at high pH. [e] Apparent third-order rate constant calculated for the **Zn_2(1)(H_2O)**-catalyzed reaction at low pH. [f] Apparent second-order rate constant for the hydroxide-ion-catalyzed reaction. [g] Rate acceleration for 1.0 M **Zn_2(1)(H_2O)** at low pH where the apparent rate constant for the **Zn_2(1)(H_2O)**-catalyzed reaction is first order in [HO^-]. [h] Stabilization of the transition state for the solution reaction at low pH by interaction with 1.0 M **Zn_2(1)(H_2O)**.

Equation 4 derived for Scheme 4 shows that this binding energy can be calculated from the ratio of the rate constants for (1) the apparent third-order rate constant for the **Zn_2(1)(H_2O)**-catalyzed reaction at low pH, where the catalyst exists mainly in the protonated form ($k_{Zn}K_a/K_w$) and where the catalyzed reaction is first-order in [HO^-] (Figure 4); this rate constant was calculated from eq 3 when $[H^+] \gg K_a$ and using $[H^+] = K_w/[HO^-]$; and (2) the second-order rate constant k_{HO} for the reaction catalyzed by hydroxide ion.

Table 2 lists the rate constants determined for the spontaneous and **Zn_2(1)(H_2O)**-catalyzed reactions of **HpPNP**, **UpPNP**, and **UpU** and the transition-state binding energies $\Delta G_{s\dagger}$ that have been calculated from these rate constants using eq 4. These transition-state binding energies are summarized in Figure 5.

Transition-State Binding Energy. There are at least three interactions between transition state and catalyst that may contribute to the stabilization of the transition state for **Zn_2(1)(H_2O)**-catalyzed cleavage of phosphate diesters: (1) Brønsted acid−base catalysis by proton transfer at the attacking nucleophilic oxygen of **HpPNP** or **UpPNP** when formation of an oxyphosphorane dianion intermediate is rate determining or to the leaving group oxygen of **UpU** when breakdown of the intermediate is rate determining;[27] (2) Interactions between the catalyst and the uridine nucleobase of **UpPNP** or **UpU**;[42−44] (3) Electrostatic interactions between the oppositely charged substrate and catalyst. We consider now the relative importance of these interactions in **Zn_2(1)(H_2O)**-catalyzed cleavage of **HpPNP**, **UpPNP**, and **UpU**.

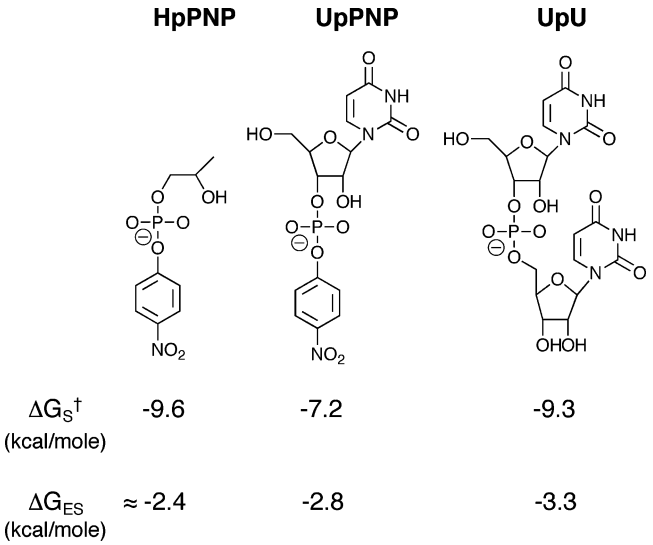

Figure 5. Comparison of the estimated changes in Gibbs free energy for formation of ground-state (ΔG_{ES}) and transition-state ($\Delta G_{S\dagger}$) complexes for the **Zn_2(1)(H_2O)**-catalyzed reactions of **HpPNP**, **UpPNP**, and **UpU**.

(1) Brønsted Catalysis. The observation of a small inverse solvent deuterium isotope effect on **Zn_2(1)(H_2O)**-catalyzed cleavage of **UpPNP** shows that there is no formal proton transfer from the C-2 hydroxyl of substrate to the catalyst at the transition state for this reaction.[23] This provides strong evidence that formal Brønsted acid−base catalysis is not significant for **Zn_2(1)(H_2O)**-catalyzed reactions when formation of an oxyphosphorane intermediate or oxyphosphorane-like transition state is rate determining.[23] It is unlikely that formal Brønsted acid−base catalysis is significant for the cleavage of **UpU**, where breakdown of an oxyphosphorane intermediate or oxyphosphorane-like transition state is rate determining. This is because similar mechanisms are expected for formation and breakdown of this intermediate/transition state in reactions that are nearly the microscopic reverse of one another. We suggested that Brønsted acid−base catalysis by **Zn_2(1)(H_2O)** is not favored because transition-state stabilization is largely due to the electrostatic interaction between the cationic catalyst and oxyphosphorane dianion.[23] A significant net stabilization of the transition state for phosphodiester cleavage by proton transfer to the nucleophile/leaving group anion is unlikely for small molecular metal ion catalysts such as by **Zn_2(1)(H_2O)** because such proton transfer will cause a decrease in negative charge at the nucleophile/leaving group and in the stabilizing electrostatic interaction between catalyst and the transition state.

(2) Interactions with Uracil Groups. There is a correlation between the number of uracil groups at the phosphate monoanion substrate and the binding affinity for **Zn_2(1)(H_2O)**. The value of $K_i = K_d = 16$ mM determined for binding of the minimal ligand dimethyl phosphate to **Zn_2(1)(H_2O)** at pH 7.6 ($\Delta G_{ES} = -2.4$ kcal/mol, Figure 5)[19,45] decreases to $K_d = 9$ mM ($\Delta G_{ES} = -2.8$ kcal/mol) and 3.5 mM ($\Delta G_{ES} = -3.3$ kcal/mol), respectively, for **Zn_2(1)(H_2O)**-catalyzed cleavage of **UpPNP** and **UpU** at pH 7.0. The increased stabilization of the complex between catalyst and substrate with increasing uracil groups suggests that this complex is stabilized by interactions between

(38) Mikkola, S.; Stemman, E.; Nurmi, K.; Yousefi-Salakdeh, E.; Stromberg, R.; Lonnberg, H. *J. Chem. Soc., Perkin Trans. 2* **1999**, 1619−1625.
(39) Wolfenden, R. *Nature* **1969**, *223*, 704−705.
(40) Pauling, L. *Nature* **1948**, *161*, 707−709.
(41) Lienhard, G. E. *Science* **1973**, *180*, 149−154.
(42) Shionoya, M.; Kimura, E.; Shirot, M. *J. Am. Chem. Soc.* **1993**, *115*, 6730−6737.
(43) Aoki, S.; Kimura, E. *J. Am. Chem. Soc.* **2000**, *122*, 4542−4548.
(44) Kimura, E.; Kitamura, H.; Ohtani, K.; Koike, T. *J. Am. Chem. Soc.* **2000**, *122*, 4668−4677.

(45) A smaller apparent inhibition constant of 11 mM for diethyl phosphate will be observed at pH 7.0 if this inhibitor binds specifically to the protonated form of the catalyst.

Scheme 5

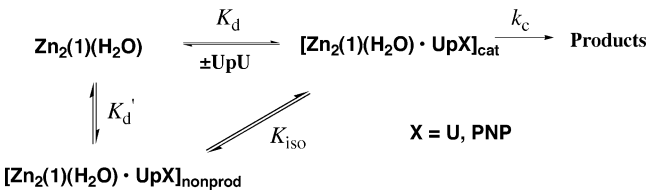

the catalyst and N-3 of the pyrimidine ring, as has been reported for analogous Zn(II) complexes.[42−44] However, these interactions are weak, and there is insufficient data to define their site at the pyrimidine ring.

On the other hand, there is no simple correlation between the magnitude of stabilization of the ground-state complexes to **Zn_2(1)(H_2O)** and of the transition state for the catalyzed cleavage reactions (Figure 5). The largest transition-state stabilization is observed for the minimal substrate **HpPNP** ($\Delta G_{S\dagger} = 9.6$ kcal/mol, Table 2) that binds most weakly to **Zn_2(1)(H_2O)**. A *weaker* transition stabilization of $\Delta G_{S\dagger} = 7.2$ kcal/mol is observed for **UpPNP**, a substrate with a single uracil group which apparently interacts with the catalyst in the ground-state complex. Finally, the 2.1 kcal/mol larger transition-state stabilization observed for the catalyzed reaction of **UpU** ($\Delta G_{S\dagger} = 9.3$ kcal/mol) compared to **UpPNP** ($\Delta G_{S\dagger} = 7.2$ kcal/mol) is greater than the 0.5 kcal/mol difference in the stabilization of ground-state complexes to the catalyst.

This difference in the effect of changing substrate structure on the ground and transition-state binding energy provides evidence that the interactions between the pyrimidine ring(s) of substrate and catalyst are expressed upon formation of a nonproductive complex between substrate and catalyst (K_d', Scheme 5) but weaken at the productive catalytic complex (K_d, Scheme 5).[46] Such nonproductive binding will cause an apparent stabilization of the Michaelis complex and a reduction in the concentration of the catalytically active complex at saturating substrate that will lead to the same proportional *decrease* in the apparent values for K_d and k_c, respectively, for the catalyzed reaction but no change in $k_c/K_d = (k_{Zn})_{app}$.[46]

We suggest that the substrates **UpPNP** and **UpU** bind to the catalyst in ground-state conformations where the interactions with the uracil ring are relatively strong and in different transition-state conformations that optimize the very strong electrostatic interactions with the oxyphosphorane dianion at the expense of weaker interactions with the uracil ring(s) (see below). This may be a general result for small molecule catalysts that show two or more *types* of stabilizing interactions with bound substrate/transition state but lack a binding pocket that shows a high lock-and-key complementarity to the transition state.

(3) Electrostatic Interactions. The following observations on the specificity of **Zn_2(1)(H_2O)** for cleavage of phosphate diesters can be rationalized by a transition state that is stabilized primarily by electrostatic interactions with the catalyst.

(1) There is a (4.4−7.2) kcal/mol increase in the stabilizing interactions between **Zn_2(1)(H_2O)** and phosphate diester ligand on proceeding from the reaction ground state to the transition state (Figure 5). This can be rationalized by an increase in electrostatic interactions between the cationic catalyst and ligands whose charge increases from −1 at the Michaelis complex to −2 at the transition state for phosphate diester cleavage.

(2) There is 2.4 kcal/mol greater stabilization of the transition state for cleavage of the minimal substrate **HpPNP** by interaction with **Zn_2(1)(H_2O)** than of the transition state for cleavage of **UpPNP** (Figure 5).[21] This is consistent with the notion that access of the more bulky substrate **UpPNP** to the charged cationic core of **Zn_2(1)(H_2O)** is restricted and that the small substrate **HpPNP** may approach more closely, allowing for stronger electrostatic stabilization of the anionic transition state.

(3) The observation that the rate-determining transition state for cleavage of **UpU** is 2.1 kcal/mol more strongly stabilized (tightly bound) by **Zn_2(1)(H_2O)** than the transition state for cleavage of **UpPNP** (Figure 5) provides evidence that the stabilizing interaction between the catalyst and the C-5′ leaving group oxyanion at the transition state for cleavage of **UpU** is stronger than the corresponding interactions between the catalyst and the nucleophilic C-2′ oxyanion at the transition state for cleavage of **UpPNP**. This conclusion will hold for either a stepwise mechanism and a pentavalent oxyphosphorane transition state or a concerted mechanism.[26,27,30,31] In either case, the barrier to expulsion of the leaving group anion will make the largest contribution to the barrier for the *uncatalyzed* cleavage of the substrate **UpU** with the strongly basic alkoxide ion leaving group, so that this site will provide a target at **UpU** for interaction with the cationic catalyst.

Catalyst Structure, Function, and Design. Effective catalysis, such as that provided by enzymes, will occur at active sites which show a high degree of complementarity to the transition state that results in strong stabilization through electrostatic, hydrogen-bonding, and hydrophobic interactions. The relatively rigid catalyst **Zn_2(1)(H_2O)** may interact with either the phosphate or the uracil fragments of substrate.[42−44] The interactions with the phosphate fragment will be expressed at the ground state for binding of the diester monoanion and strengthen on proceeding to the transition-state oxyphosphorane dianion. The interactions between **Zn_2(1)(H_2O)** and the N3 of the uracil group will also be expressed at the ground-state complex. However, these interactions may be nonproductive (Scheme 5) if they are weakened by a reorientation of the ground-state complex on proceeding to a reaction transition state that gives optimal electrostatic interactions between the cationic core of the catalyst and the oxyphosphorane dianion.

There are several advantages of modular small molecule and enzyme catalysts with domain(s), connected by a flexible linker-(s), that interact with different substrate fragments, over catalysts with a rigid structure. (1) It is simpler to design such a flexible catalyst that explores many conformations to find the one providing maximum transition-state stabilization than a catalyst of a single fixed structure that provides the same enthalpic transition-state stabilization. (2) It will be difficult to change the substrate specificity for a rigid catalyst because changes in structure that modify the binding specificity at one domain may also adversely affect the binding interaction at other domains. The interdependence of interactions at such domains will be reduced for a modular catalyst where they are free to move independently, so as to maximize the binding interactions at each. This will favor rapid evolution of new enzyme activi-

(46) Fersht, A. R. *Structure and Mechanism in Protein Science*; W. H. Freeman and Co.: New York, 1999; pp 114−118.

ties.[47,48] (3) Conformational flexibility that reversibly exposes the active site to bulk solvent is required for the large number of enzymes that encapsulate their bound substrate(s).[49]

Effective catalysis of phosphate diester cleavage may be obtained by tethering a cationic core to a nucleoside recognition element, provided the tether allows sufficient conformational flexibility for both groups to show optimal binding interactions with their targeted regions of the substrate. A simple example of this strategy that is being pursued in a number of laboratories is the tethering of a metal ion complex to a short sequence of antisense RNA that is complementary to a strand of messenger RNA that has been targeted for cleavage.[50−54]

Acknowledgment. J.R.M. and J.P.R. thank the National Science Foundation (CHE9986332) for support of this work.

JA056167F

(47) Wise, E. L.; Yew, W. S.; Akana, J.; Gerlt, J. A.; Rayment, I. *Biochemistry* **2005**, *44*, 1816−1823.
(48) Yew, W. S.; Akana, J.; Wise, E. L.; Rayment, I.; Gerlt, J. A. *Biochemistry* **2005**, *44*, 1807−1815.
(49) Richard, J. P.; Amyes, T. L. *Bioorg. Chem.* **2004**, *32*, 354−366.
(50) Magda, D.; Wright, M.; Crofts, S.; Lin, A.; Sessler, J. L. *J. Am. Chem. Soc.* **1997**, *119*, 6947−6948.
(51) Canaple, L.; Husken, D.; Hall, J.; Haner, R. *Bioconjugate Chem.* **2002**, *13*, 945−951.
(52) Astrom, H.; Williams, N. H.; Stromberg, R. *Org. Biomol. Chem.* **2003**, *1*, 1461−1465.
(53) Baker, B. F.; Lot, S. S.; Kringel, J.; Cheng-Flournoy, S.; Villiet, P.; Sasmor, H. M.; Siwkowski, A. M.; Chappell, L. L.; Morrow, J. R. *Nucleic Acids Res.* **1999**, *27*, 1547−1551.
(54) Baker, B. F.; Khalili, H.; Wei, N.; Morrow, J. R. *J. Am. Chem. Soc.* **1997**, *119*, 8749−8755.